Design and Simulation of Low Cost and Low Magnetic Field MRI System

Sweta Ghosh, Vikram Thakur, Rahul Shrestha,
Shubhajit Roy Chowdhury
Biomedical Systems Laboratory, MANAS Group
School of Computing and Electrical Engineering,
Indian Institute of Technology Mandi,
Mandi, India
Emails: sweta_karmakar@students.iitmandi.ac.in,
vikram.th07@gmail.com,
rahul_shrestha@iitmandi.ac.in, src@iitmandi.ac.in

Vinayak Hande
Department of Electrical Engineering,
Indian Institute of Technology Ropar,
Rupnagar, India
Email: vinayak.hande@iitrpr.ac.in

Abstract— **We present the design of a Magnetic Resonance Imaging (MRI) system based on Helmholtz coil in place of a permanent magnet which is common in commercial MRI systems. Inspired by the homogeneity of the magnetic field of the Helmholtz coil, the design has been proposed. This coil generates a main magnetic field of 0.2T which is a low magnetic field and hence it was possible to make the system low weight to some extent. This makes the proposed design suitable to be taken and operated at remote locations. Along with the main magnetic field, other components are also necessary like the gradient coils, radio-frequency coils and a constant DC current source, to mention a few. The gradient has strength of 75µT/m. The resonating frequency at which the radio-frequency operates is 8.256MHz for 0.2T and the DC source gives a current of 10A with 50V DC which is essential requirement for the operating of the coils. All the components taken together make the whole system.**

Keywords - Helmholtz coil; Maxwell coil; RF coil; constant DC source; homogeneity; magnetic field.

I. INTRODUCTION

Magnetic Resonance Imaging (MRI) is a medical imaging method used in radiology to form images of the biological processes of body in both health and disease conditions. MRI, also known as nuclear magnetic resonance imaging, is a technique for creating images of external as well as internal organs of human body. MRI scanners enable fast, non-invasive, and high-resolution imaging of organs and soft tissue.

MRI was established as a promising diagnostic tool in the beginning of 1980s. While high magnetic field ($\geq$ 1.0T) MRI scanners continue to be the most commonly used, there is growing interest in the utilization of low-field ($\leq$ 0.5T) extremity scanners [6]. They are smaller, less expensive, and easier to install, and allow for quicker patient diagnoses in an office setting. In contrast, high magnetic field scanners have superior image quality because of higher signal-to-noise ratio (SNR), contrast, and resolution [1]. It is possible for low-field scanners to improve image quality by increasing scan duration, although doing so also increases the chance of motion artifacts [1]–[4] While lowfield MRI images may not be able to compete with the quality of those produced using high-field scanners, it is important to consider whether or not they can provide comparable diagnostic capabilities to justify their logistical benefits. When compared with surgical findings, the use of low-field extremity MRI scanners for identifying medical meniscus pathology has

been promising (sensitivity, 77%-96%; specificity, 71%-100%); however, the results for identifying pathology of the lateral meniscus have been more variable [5]–[13]. Most of these studies show low-field MRI to be a moderately good identifier of sub-peripheral and meniscus pathology (sensitivity, 75%- 93%; specificity, 94%-100%).

Ghazinoor et al. concluded that their subjective experience is in concordance with many studies demonstrating the high diagnostic value in the use of low-field scanners in musculoskeletal pathology [1]. Tavernier et al. stated that the primary limitation of low-field MRI is lower SNR, which has to be compensated for by increasing the slice thickness, reducing the in-plane resolution, increasing the number of acquisitions (and consecutively the acquisition time), and decreasing the bandwidth [14].

Tavernier et al. concluded that implementation of low-field MRI systems may be useful, especially in orthopaedic centers, or if installation of an additional high-field scanner is not possible because of economic considerations [14]. Blanco et al showed that there is trade-off in image quality towards less resolution due to open structure of these systems [15]. The image quality of low-field scanners is, however, sufficient for interventional use. In a review article, Hayashi et al. noted that no reliable efficacy studies, however, exist comparing the diagnostic capabilities of low- versus high-field scanners [16]. In order to compensate for lower SNR, scanners with low field strength tend to have longer acquisition times, often resulting in greater image degradation due to patient movement.

The current research focuses on the development of a low cost and low magnetic MRI machine for the point of ease testing support. In order to provide the diagnostics support at the point of care, the MRI is proposed to sufficient small weight, because of which Helmholtz coil instead of permanent magnetic is proposed to be used to generate the main magnetic field. The gradient coil is implemented with Maxwell coil. The RF coil design has been implemented based on the papers of Mehmet Bilgen in 2004 and 2001[21-22]. Their study showed implantable coils can work fine having good SNR.

The paper is divided in the following sections. Section II focuses on the design of material and method, Section III discusses the design of the different coils (Helmholtz coil, Maxwell coil; RF coil which has done using concept of COMSOL Multiphysics 5:2 and CST), Section IV discusses results, and Section V the discussion. Section VI concludes the paper.

II. MATERIALS AND METHODS

The MRI in the proposed design is based on Helmholtz Coil. Hence, the main magnetic field is generated using the above mentioned coil. The main magnetic field is of 0.2 T. For such a low magnetic field, the gradient strength is kept at 75μT/m. The gradient fields are necessary to obtain the spatial information about the subject. Maxwell Coil and Saddle Coil were designed as the gradient coils. All these coils are concentric. The inner radius of the system is 40cm, which is enough for head or limbs to be inserted. The inner radius is the radius for the radio-frequency (RF) coil which is a surface coil for the time being.

All the coils are built with annealed copper. For the coils, copper wires were used with AWG gauge size of 11 (2.303mm diameter). Since RF coil is a surface coil it's designed on PCB (Printed Circuit Board) using annealed copper.

III. DESIGN OF COILS

A. Design of Helmholtz Coil

Helmholtz coil is basically a pair of coils that are separated from each other at a distance equal to the radius of the coil. The magnetic field is calculated applying Biot Savart's law for Helmholtz Coil. According to Biot Savart's Law,

$$B_1(x) = \frac{\mu_0 n I R^2}{\left(R^2 + x^2\right)^{\frac{3}{2}}} \tag{1}$$

where μ_0 is the permeability constant $= 4\pi \times 10^{-7}$ Tm/A. I is the current in the coil. R is the radius of the coil and x is the distance of a point from the coil on the axis of the coil and n is the number of turns of the coil. $B_1(x)$ is the magnetic field generated along the axis of the coil due to current I.

In case of Helmholtz coil the Biot Savart's Law gets modified a little. In a Helmholtz Coil, a point that is halfway between the coils has a value of x equal to $R/2$. The magnetic field at that point due to the two coils is given by,

$$B_1\left(\frac{R}{2}\right) = \left(\frac{8}{5\sqrt{5}}\right)\frac{\mu_0 n I}{R} \tag{2}$$

Since the main magnetic field was 0.2T and the radius was taken to be 30 cm or 0.3 m, so for a current of 10A the number of turns for each coil was obtained as 6675. The orientation of the coil is shown in Figure 1.
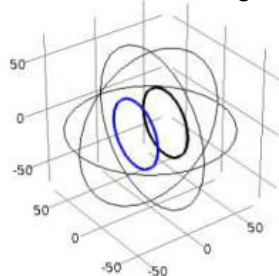
Figure 1. Helmholtz Coil pair of radius 30cm

It is necessary that the main magnetic field be uniform over the volume of interest. Hence, homogeneity becomes one of the important aspects for the main magnetic field or Helmholtz Coil. Homogeneity is calculated from the center of the coil to any particular point and it is measured in percentage change of magnetic field strength from center to any particular point.

$$H(\%) = \frac{\left(B_i - B_0\right)}{B_0} \times 100\% \tag{3}$$

H is the homogeneity or percentage change of magnetic field strength at any point from the center. B_i is the magnetic field at any point in the volume and B_0 is the magnetic field at the center. Generally volumes of spheres or cylinders are considered to specify homogeneity. Here a sphere has been chosen to calculate homogeneity in the Helmholtz coil. From the homogeneity, the region of study can be predicted very well, thus defining the area where to place the patient.

B. Design of Gradient Coils

Gradient coils provide some deliberate inhomogeneities which can be used to frequency encode spatial information of the signal returned by the sample or subject. Maxwell coil and Saddle coil has been used as the gradient coils. While Maxwell coil provide the gradient field along the z axis (longitudinal gradient), Saddle coils provide the gradient strength along the x and y axis (transverse gradients) respectively. The basic equation governing the linearly varying the gradient magnetic field is given by,

$$B_Z(x,y,z) = B_0 + \frac{\partial B_z}{\partial x}x + \frac{\partial B_z}{\partial y}y + \frac{\partial B_z}{\partial z}z$$
$$= B_0 + G_x x + G_y y + G_z z \tag{4}$$

where B_0 is the main magnetic field. G_x and G_y are the transverse gradient and G_z is the longitudinal gradient. Maxwell coil is governed by the equation,

$$B_Z = \frac{\mu_0 I a^2}{2\left[\left(\frac{d}{2} - z\right)^2 + a^2\right]^{\frac{3}{2}}} - \frac{\mu_0 I a^2}{2\left[\left(\frac{d}{2} + z\right)^2 + a^2\right]^{\frac{3}{2}}} \tag{5}$$

Here, B_z is the magnetic field along the z axis due to the current in the coils. μ_0 is the permeability constant, I is the current in coil (in Amperes), a is the radius of coil (in meters) and z and d are the distance of a point from the coil on the axis (in meters) and the distance between the coils respectively. A gradient strength of 75μT/m has been considered having a current of 5A in a coil of radius 25 cm. The orientation of Maxwell coil is shown in Figure 2.
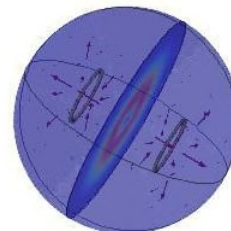
Figure 2. Maxwell coil orientation and magnetic lines of force

The transverse gradient i.e. gradients in the *x* and *y* directions is obtained from the basic equation,

$$B_Y(y,z) = \frac{\mu_0 I}{2\pi}\left[\frac{b-y}{(b-y)^2 + (d-z)^2}\right] \quad (6)$$

B_z represents the gradient field along *y* direction and *b* and *d* are the co-ordinates in the *yz* plane. For *x* direction the Saddle coil is rotated 90degrees.

C. Design of Radio-Frequency Coil

The radio-frequency (RF) radiation on the magnetization of the sample is important to obtain images. The RF coil consists of a transmitter and receiver section. The transmitter section radiates the sample with a RF field in order to tip the magnetization away from equilibrium position and that it can generate a detectable NMR signal. The receiver section receives the signal and transforms the signal from analog to digital using some necessary circuitry.

The protons in the subject or patients go from one energy state to another energy state by releasing energy. That is they emit photon of some frequency to move from an excited state to equilibrium state. This frequency is directly proportional to the magnetic field strength. The relation between the resonating frequency and the main magnetic field is given by,

$$\varpi = \gamma B_0 \quad (7)$$

where ϖ is the angular frequency, B_0 is the main magnetic field and is the gyromagnetic ratio for protons whose value is 42.58 MHz/T. From the fact that main magnetic field is 0.2T the resonating frequency comes out to be 8.526MHz. This frequency is also called the Larmor frequency of the nucleus. For designing the coil, it is required take the length of the coil less than the wavelength. The length of the wire was taken at $1/20^{th}$ of the wavelength which is 1.76m. The design is simple rectangular spiral coil (surface coil) whose dimension is 20cm by 10cm.

D. Design of Constant DC source

The voltage-mode feedback approach in circuit design is becoming more common; because circuits designed using this approach will always work better at low speed-high accuracy, than its current-mode counterpart. Therefore many systems could take advantage of voltage-mode feedback over a wide field of applications like low frequency voltage or current reference design.
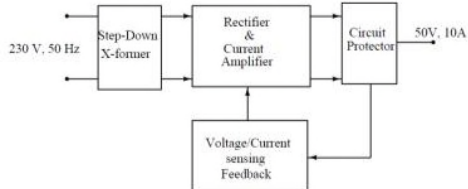
Figure 3. Block diagram of constant DC current source

The block diagram of constant DC current source is shown in Figure 3. Step down transformer converters 230V, 50Hz mains power supply to 50V, 50Hz. Rectifier convert it into DC voltage. Later sensing feedback makes sure that the output voltage and currents are 50V (DC) and 10A (DC), respectively.
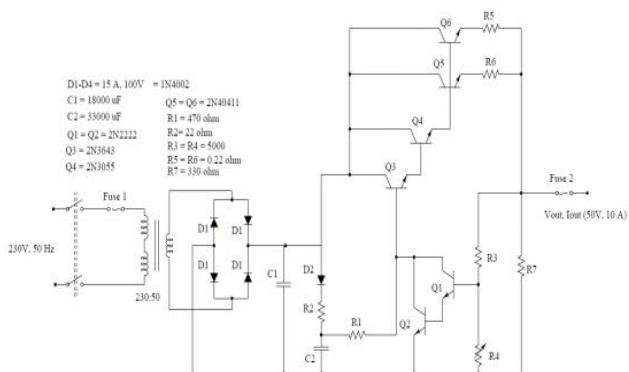
Figure 4. Circuit diagram of constant DC current source

Circuit diagram of constant DC current source is shown in Figure 4. Rectifier contains bridge type rectifier with large value capacitor. Sensing and feedback circuit consist of resistors R3 and R4 along with two Darlington BJT pairs of Q1-Q2 and Q3-Q4. The feedback factor in terms of voltage is given in eq. 8.

$$feedback(V) = I_{B_1}\left(\frac{R_4 R_7}{R_3 + R_4}\right)(\beta_5 + \beta_6)(\beta_1\beta_2\beta_3\beta_4) \quad (8)$$

By selecting larger values of beta's (β), the feedback factor can be increased. However, large power rating along with large beta BJTs increases the cost further.

IV. RESULTS

The simulations were performed in COMSOL Multiphysics and CST (Computer Simulation Technology). In both softwares, a 3-Dimensional design is provided, material is also assigned and also the study type is given. The results are discussed in the subsections.

A. Simulation of Helmholtz Coil

The model of Helmholtz Coil has been built in COMSOL Multiphysics. The coil was designed for a magnetic field strength of 0.2T. The inner radius of the coil has been kept 30 cm or 0.3 m while the outer radius extends upto 59 cm. The material of the coil was copper having a gauge size of 11. Using the equation of the magnetic field the number of turns obtained was 6675 for a current of 10A. Having considered these specifications the magnetic flux density was obtained from the simulation. The results are shown in Figure 5 below.
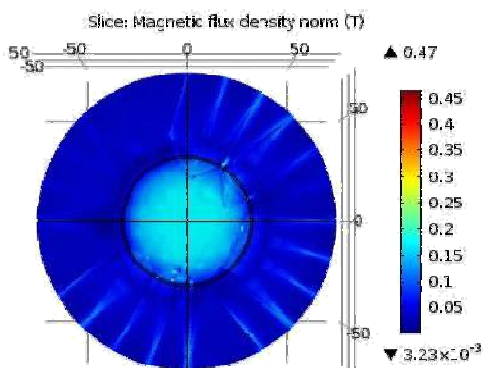
Figure 5. Magnetic flux density at the center of the coil.

Homogeneity of Helmholtz Coil is considered to be uniform i.e. magnetic field is uniform within the coil. The uniformity of the coil can be observed from the figure above. Also, a line graph has been obtained from the simulation as shown in Figure 6.
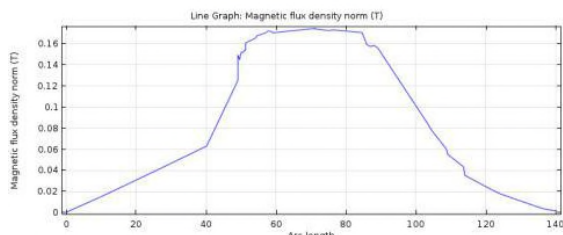
Figure 6. Homogeneity of Helmholtz coil

B. Simulation of Maxwell Coil

Maxwell Coil is anti-Helmholtz coil whose governing equation has been given above. Maxwell Coil has been used for longitudinal gradient and Saddle coil has been used for transverse gradient. In Maxwell coil the distance between the coils is $\sqrt{3}$ times the radius of the coil. The radius of the coil has been taken as 25 cm and the current 5A. Having these specifications the number of turns obtained was 125 and the slope or gradient strength was 75µT/m. The slope was determined from this graph in Figure 7.
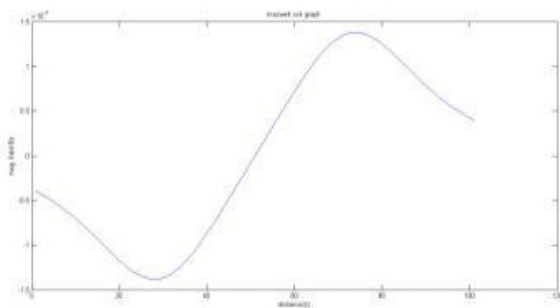
Figure 7. Slope of the Maxwell coil

The simulation result in Figure 8 shows the distribution of magnetic flux density of the Maxwell coil. The magnetic flux varies from the center towards outside.
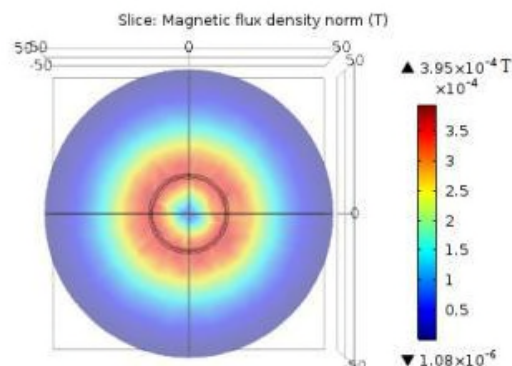
Figure 8. Magnetic flux distribution of Maxwell coil

C. Simulation of RF coil

When it comes to radio-frequency coil (RF coil), it is one of the important part of the MRI system. The RF coil is responsible for images developed from a MRI system. The RF coil consists of two parts, the transmitter part and the receiver part. Both these parts are designed separately. A basic design of the transmitter part is given in Figure 9. It simply consists of a rectangular spiral coil which was simulated in Computer Simulation Technology (CST). The model is shown in Figure 9.
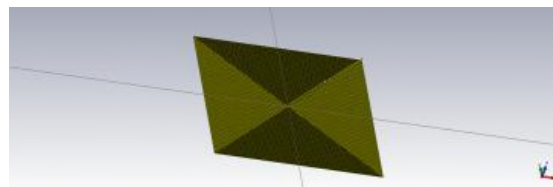
Figure 9. Model of simple transmitter part

The magnetic field and the electric field generated by this model are shown in Figures 10 and 11, respectively.
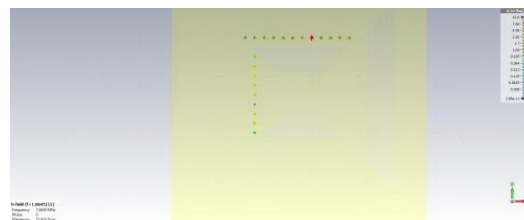
Figure 10. Magnetic field by the transmitter part
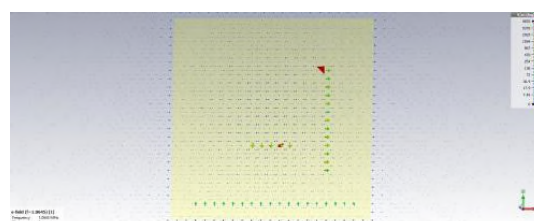
Figure 11. Electric field of the transmitter part

D. Experimental setup of constant DC source

Figure 12. Measurement set-up for constant DC current source

Measurement set-up is shown in Figure 12. Input single phase- secondary's AC is recorded i.e. 45 V. Output DC voltage (50 V : clearly visible) and DC current (10 A : little hazy) are shown here. Due to large value capacitor we get 50V DC after applying 45 V AC as input. The outputs are observed to be constant at 10A with 50V DC. This circuit is useful as voltage and current reference circuit for powering up the low cost MRI systems.

V. DISCUSSION

The various results are obtained from COMSOL Multiphysics5.2 for single slice and multi-slice in multidomain and X-Y plane. The results show the distribution of magnetic field in coil, surface charge density of the coils and percentage of homogeneity of magnetic field at the centre of the two coils. Helmholtz coil and Maxwell coil have these results. The simulation results give insights on placement of the subject inside the MRI machine for MR imaging. Figure 3 shows the inner side edge of second coil, which the reference edge is taken for Helmholtz coil from where we started our studies. However in the RF coil, studies were performed in CST. In that simple design results were obtained for 1V input voltage. And the output for the constant DC current source is observed to be 10A with 50 V DC.

A. Helmholtz coil and Maxwell coil

Simulation studies regarding the Helmholtz coil as well as the Maxwell coil shows the distribution of magnetic flus density of the coils. Regarding the Helmholtz coil the flux density was found to be 0.2T (calculated and simulated). For the Maxwell coil, the flux density is zero at the center of the coil, which is also depicted by the simulation result. From the flux density graph in figure and the homogeneity graph in figure it can clearly be inferred that the field is homogeneous within the coil. The flux density is constant within some region of the coil (region of study) inferring that field is homogenous in that region.

A study of homogeneity along the radial length of the coil is given in TABLE I. And it can be seen that homogeneity lies within ±2% in the region of study.

B. RF coil

The design of RF coil is simple rectangular spiral coil. And it's electric and magnetic field has been shown in Figures 8 and 9. Using these two fields the RF coil can be easily designed. A magnetic field of 1.3T is within the coil and an electric field of 867 V/m is within the coil.

C. Constant DC current source

An input of 45 V at the single phase secondary's AC is recorded while at the output DC voltage 50 V is recorded. A DC current of 10A with 50 V is observed at output.

TABLE I. HOMOGENEITY OBTAINED FROM SIMULATION OF HELMHOLTZ COIL

Radius (cm)	Homogeneity (%)
4.29	0.33
11.5	0.48
11.85	0.47
12.9	1.8
14.53	2.63
25.85	39

D. Comparison with existing MRI systems available in literature

The cost and performance of the proposed MRI system has been compared with MRI systems available in literature and presented in TABLE II.

TABLE II. COMPARISON OF PROPOSED MRI WITH MRI AVAILABLE IN LITERATURE

Type of MRI	Cost/Estimated Cost	Homogeneity of magnetic field	Weight of the system
Proposed MRI	INR 10 lacs	1%	2 tons
Esaote® MRI [23]	INR 2.5 crores	0.8%	15 tons

The results shown in TABLE II clearly indicate that except for a marginal loss in homogeneity, there is a tremendous reduction in cost and weight of the MRI system which will prove beneficial for the implementation of a low cost transportable MRI system in a developing country like India.

VI. CONCLUSION

This paper presents a design of Helmholtz coil, Gradient coil, RF coil and constant DC current source for the development of a low cost and low magnetic field MRI system. The simulation results have been obtained for Helmholtz coil and Maxwell coil in z-direction for magnetic flux density, magnetic field at the centre of the coil and over the surface of the coils obtained from COMSOL Multiphysics 5.2. The RF coil was simulated in CST environment to obtain the electric field and the magnetic field which gave a rough idea regarding the design of RF coil. The plots obtained from the COMSOL and our calculated data shows the exact same values prove that our approach is accurate. Our study reveals that there occurs homogeneity in Helmholtz coil where we can place subject for study. We have calculated and validated through simulation that homogeneity at the centre of Helmholtz coil is about ±2 per cent over the region of study. The constant DC source gave an output of 10A with 50 V which is our requirement. This machine will be useful and harmless for mankind and will give the better results as compared to bulky machines.

REFERENCES

[1] S. Ghazinoor and J. V. Crues, "Low field mri: a review of the literature and our experience in upper extremity imaging," Clinics in sports medicine, vol. 25, no. 3, pp. 591–606, 2006

[2] S. Ghazinoor, J. V. Crues, and C. Crowley, "Low-field musculoskeletal mri," Journal of Magnetic Resonance Imaging, vol. 25, no. 2, pp. 234–244, 2007.

[3] R. Loew, K. Kreitner, M. Runkel, J. Zoellner, and M. Thelen, "Mrarthrography of the shoulder: comparison of low-field (0, 2 t) vs highfield (1.5 t) imaging," European radiology, vol. 10, no. 6, pp. 989–996,2000.

[4] K. Woertler, M. Strothmann, B. Tombach, and P. Reimer, "Detection of articular cartilage lesions: Experimental evaluation of low-and highfield-strength mr imaging at 0.18 and 1.0 t," Journal of Magnetic Resonance Imaging, vol. 11, no. 6, pp. 678–685, 2000.

[5] M. J. Barnett, "Mr diagnosis of internal derangements of the knee: effect of field strength on efficacy." AJR. American journal of roentgenology, vol. 161, no. 1, pp. 115–118, 1993.

[6] A. Cotten, E. Delfaut, X. Demondion, F. Lap`egue, M. Boukhelifa, N. Boutry, P. Chastanet, and F. Gougeon, "Mr imaging of the knee at 0.2 and 1.5 t: correlation with surgery," American Journal of Roentgenology, vol. 174, no. 4, pp. 1093–1097, 2000.

[7] F. Sp, W. Del Pizzo, F. Mj et al., "Accuracy of diagnoses from magnetic resonance imaging of the knee," Clinical Journal of Sport Medicine, vol. 1, no. 3, p. 212, 1991.

[8] J. L. Glashow, R. Katz, M. Schneider, and W. Scott, "Double-blind assessment of the value of magnetic resonance imaging in the diagnosis of anterior cruciate and meniscal lesions." J Bone Joint Surg Am, vol. 71, no. 1, pp. 113–119, 1989.

[9] J. Kinnunen, S. Bondestam, A. Kivioja, J. Ahovuo, S.Toivakka, I. Tulikoura, and T. Karjalainen, "Diagnostic performance of low field mri in acute knee injuries," Magnetic resonance imaging, vol. 12, no. 8, pp. 1155–1160, 1994.

[10] H. S. Lokannavar, X. Yang, and H. Guduru, "Arthroscopic and lowfield mri (0.25 t) evaluation of meniscus and ligaments of painful knee," Journal of clinical imaging science, vol. 2, 2012.

[11] B. R. Mandelbaum, G. A. Finerman, M. A. Reicher, Hartzman, L. W. Bassett, R. H. Gold, W. Rauschning, and F. Dorey, "Magnetic resonance imaging as a tool for evaluation of traumatic knee injuries anatomical and pathoanatomical correlations," The American journal of sports medicine, vol. 14, no. 5, pp. 361–370, 1986.

[12] K.-A. Riel, M. Reinisch, B. Kersting-Sommerhoff, N. Hof, and T. Merl, "0.2-tesla magnetic resonance imaging of internal lesions of the knee joint: a prospective arthroscopically controlled clinical study," Knee Surgery, Sports Traumatology, Arthroscopy, vol. 7, no. 1, pp. 37–41, 1999.

[13] R. T. Blanco, R. Ojala, J. Kariniemi, J. Per¨al¨a, J. Niinim¨aki, and O. Tervonen, "Interventional and intraoperative mri at low field scanner– a review," European journal of radiology, vol. 56, no. 2, pp. 130 142, 2005.

[14] T. Tavernier and A. Cotten, "High-versus low-field mr imaging," Radiologic clinics of North America, vol. 43, no. 4, pp. 673–681, 2005.

[15] N. Hayashi, Y. Watanabe, T. Masumoto, H. Mori, S. Aoki, K. Ohtomo, O. Okitsu, and T. Takahashi, "Utilization of low-field mr scanners," Magnetic resonance in medical sciences, vol. 3, no. 1, pp. 27– 38, 2004.

[16] H. Yoshioka, S. Ito, S. Handa, S. Tomiha, K. Kose, T. Haishi, A. Tsutsumi, and T. Sumida, "Low-field compact magnetic resonance imaging system for the hand and wrist in rheumatoid arthritis," Journal of Magnetic Resonance Imaging, vol. 23, no. 3, pp. 370–376, 2006.

[17] A. K. Scheel, K. A. Hermann, S. Ohrndorf, C. Werner, C. Schirmer, J. Detert, M. Bollow, B. Hamm, G. A. M¨uller, G. R. Burmester et al., "Prospective 7 year follow up imaging study comparing radiography, ultrasonography, and magnetic resonance imaging in rheumatoid arthritis finger joints," Annals of the rheumatic diseases, vol. 65, no. 5, pp. 595– 600, 2006.

[18] B. Ejbjerg, E. Narvestad, M. Szkudlarek, J. Jacobsen, "Öptimised low cost low-field dedicated extremity mri can provide similar information on wrist and mcp joint synovitis and bone erosions as expensive conventional high-field mri arthritis-a comparison with conventional'high-field mri," in Ann Rheum Dis, 2002.

[19] J. V. Crues, F. G. Shellock, S. Dardashti, T. W. James, and O. M. Troum, "Identification of wrist and metacarpophalangeal joint erosions using a portable magnetic resonance imaging system compared to conventional radiographs." The Journal of rheumatology, vol. 31, no. 4, pp. 676–685, 2004.

[20] H. Lindegaard, J. Vallø, K. Hørslev-Petersen, P. Junker, and M. Østergaard, "Low field dedicated magnetic resonance imaging in untreated rheumatoid arthritis of recent onset," Annals of the rheumatic diseases, vol. 60, no. 8, pp. 770–776, 2001.

[21] M. Bilgen, "Simple low cost multipurpose RF coil for MR microscopy at 9.4 T", Magnetic Resonance in Medicine, Vol, 52, pp. 937 – 940, 2004.

[22] M. Bilgen, I. Elshafiey, and P. A. Narayana, " In vivo magnetic resonance microscopy of rat spinal cord at 7 T using implantable RF coils", Magnetic Resonance in Medicine, Vol, 46, pp. 1250 – 1253, 2001.

[23] https://www.esaote.com/en-IN/dedicated-mri/mri-systems/p/s-scan/ [accessed August 2018]